Two–Dimensional Iterative APP Channel Estimation and Decoding for OFDM Systems

Stephan ten Brink, Frieder Sanzi, Joachim Speidel

Abstract— **We present a channel estimation method for coherent detection of multicarrier signals which is based on the A Posteriori Probability calculation algorithm (APP estimator). A two–dimensional channel estimation is performed by applying a concatenation of two one–dimensional APP estimators. The combination with an outer soft in/soft out channel decoder allows to further improve the bit error rate by means of iterative estimation and decoding. The robustness of the new channel estimator permits to reduce the number of pilot symbols which are required as phase references for coherent detection. It is readily applicable to current multicarrier systems (e.g. DVB–T) without changing the transmission format. A combination with an inner convolutional code is suggested to further improve performance.**

Keywords— **multicarrier modulation, channel estimation, iterative decoding**

I. Introduction

The time–varying propagation conditions of the mobile communication channel make channel estimation for multicarrier systems a demanding task at the receiver. To allow for coherent detection, the two–dimensional channel transfer function must be estimated. For this, pilot symbols are periodically inserted into the transmitted signal. The channel estimation is typically performed by applying a two–dimensional FIR interpolation filter whose coeffients are based on the Wiener design criterion, as described e. g. in [1].

In [2] the authors propose a modified A Posteriori Probability calculator (APP or MAP algorithm, [3]) for the purpose of joint channel estimation and differential detection of DPSK–signals in frequency non–selective (flat) Rayleigh fading channels. In this paper we extend the idea of APP estimation to the two–dimensional multicarrier scenario. In particular, we use a concatenation of two one–dimensional APP estimators in time and frequency direction to perform an estimation of the two–dimensional channel transfer function. This enables iterative estimation and decoding at the receiver to further reduce the bit error rate (BER). A combination with an inner recursive convolutional code is shown. The proposed channel estimation algorithm requires less pilot symbols to achieve the same bit error rate and is more robust against a change in the statistics of the mobile communication channel than conventional methods.

The authors are with the Institute of Telecommunications, Dep. 0408, University of Stuttgart, Pfaffenwaldring 47, 70569 Stuttgart, Germany. Tel: +49 711 685 7937, Fax: +49 711 685 7929, E-mail: {tenbrink, sanzi, speidel}@inue.uni-stuttgart.de . Part of this work has been performed in a joint project with Bell Laboratories, Lucent Technologies.

II. System Model

A. Transmitter

The signal from the binary source is convolutionally encoded, interleaved, serial to parallel converted and modulated (BPSK) onto N orthogonal sub–carriers by an iFFT–block (Fig. 1). Additionally, pilot symbols are periodically inserted to allow for coherent detection at the receiver. The transmission is done on a block–by–block basis, with blocks of N sub–carriers in frequency and K OFDM–symbols in time direction.

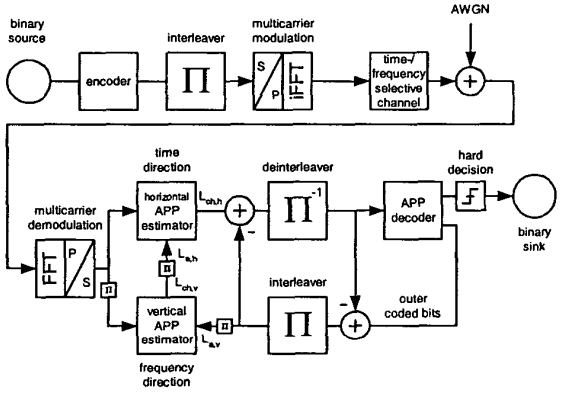

Fig. 1. System configuration with transmitter, channel and decoder.

B. Channel Model

For the mobile communication channel we apply the wide–sense stationary uncorrelated scattering (WSSUS) channel model as given in [4].

$$H(t,f) = \frac{1}{\sqrt{L}} \cdot \sum_{i=0}^{L-1} \exp\left[j\left(\varphi_i + 2\pi\left(f_{D,i} \cdot t - \tau_i \cdot f\right)\right)\right] \quad (1)$$

The variable L denotes the number of propagation paths; the phase φ_i is uniformly distributed, the delay spread τ_i exponentially distributed with probability density function (PDF) $p(\tau)$; $f_{D,i}$ is distributed according to Jakes' power spectral density. The auto–correlation function in time is $R_{t;k} = J_0\left(2\pi f_{D,max} \cdot k \cdot T_s\right)$; T_s is the duration of one OFDM symbol, k the discrete time index and $f_{D,max}$ the maximal Doppler shift. The complex auto–correlation function in frequency direction writes as

$$R_{f;n} = \frac{1 - \exp\left[-\tau_{max}\left(\frac{1}{\tau_{rms}} + j2\pi \cdot n \cdot \Delta f\right)\right]}{\left(1 - \exp\left[-\frac{\tau_{max}}{\tau_{rms}}\right]\right) \cdot \left(1 + j2\pi \cdot n \cdot \Delta f \cdot \tau_{rms}\right)} \quad (2)$$

0-7803-6451-1/00/$10.00 © 2000 IEEE

IEEE Global Communications Conference (GLOBECOM), San Francisco (USA), Nov. 2000, 741-745

with τ_{rms} chosen such that $p(\tau_{max})/p(0) = 1/1000$; τ_{max} is the channel delay spread, Δf the sub–carrier spacing, and n the discrete frequency index.

C. Receiver

After demodulation of the N sub–carriers and parallel to serial conversion, the signal is fed to the channel estimation stage. Different variations of the APP estimation algorithm are used which are explained in more detail in Section III. The APP estimation includes pilot symbol extraction and channel weighting for coherent detection. The APP estimator outputs log–likelihood ratios (L–values [5]) on the transmitted coded bits which are deinterleaved and decoded in an soft in/soft out (APP) channel decoder. Iterative channel estimation and decoding is performed by feeding back "outer extrinsic information" on the coded bits; after interleaving it becomes the *a priori* knowledge to the APP estimation stage.

III. Channel estimation with a priori knowledge

For APP estimation, the symbol–by–symbol MAP–algorithm according to [3] is applied to an appropriately chosen metric. For this, the transmitted coded bits can be thought of being put into a virtual shift register at the output of the transmitter. This "artifical grouping" allows to exploit the time and frequency continuity of the channel transfer function at the receiver by trellis processing [6]. Note that each sub–carrier experiences only flat fading. The received symbol from the channel at discrete time k, $0 \le k < K$ and discrete frequency (i. e. sub–carrier index) n, $0 \le n < N$ is $z_{k,n} = a_{k,n} \cdot x_{k,n} + n_{k,n}$, with $a_{k,n} = H(t = kT_s, f = n\Delta f)$ being the complex fading coefficient as obtained from (1), $x_{k,n}$ being the transmitted binary symbol $x_{k,n} \in \{\pm 1\}$ and $n_{k,n}$ the complex additive white Gaussian noise with component–wise noise power $\sigma_n^2 = N_0/2$.

A. One–dimensional APP estimators

At frequency index n (time index k omitted), the logarithmic metric increment of the vertical APP estimation (frequency direction, BPSK–modulated signals) can be simplified to

$$\gamma_n = \frac{\mathrm{Re}\left\{z_n \cdot \hat{x}_n \cdot \hat{a}_{v,n}^*\right\}}{\sigma_{v,pred}^2} + \tfrac{1}{2} L_{a,v,n} \tag{3}$$

with estimated channel coefficient (linear FIR–prediction of order m_v)

$$\hat{a}_{v,n} = \sum_{i=1}^{m_v} c_{v,i} \cdot z_{n-i} \cdot \hat{x}_{n-i} \tag{4}$$

whereby the vertical FIR–filter coefficients $c_{v,i}$ are calculated with the Wiener–Hopf equation based on the frequency auto–correlation of the channel transfer function. The variable z_n denotes the received channel observation at frequency index n (and time index k), $\hat{x}_n \in \{\pm 1\}$ the hypothesized transmitted bits according to the trellis structure, $L_{a,v,n}$ the vertical *a priori* L–values and $\sigma_{v,pred}^2$ the variance of the vertical estimation error. The asterisk "*" is the complex–conjugate operator.

Accordingly, at time index k (frequency index n omitted), the horizontal APP estimation (time direction) is characterized by the metric increment

$$\gamma_k = \frac{\mathrm{Re}\left\{z_k \cdot \hat{x}_k \cdot \hat{a}_{h,k}^*\right\}}{\sigma_{h,pred}^2} + \tfrac{1}{2} L_{a,h,k} \tag{5}$$

with estimated channel coefficient

$$\hat{a}_{h,k} = \sum_{i=1}^{m_h} c_{h,i} \cdot z_{k-i} \cdot \hat{x}_{k-i} \tag{6}$$

whereby the horizontal FIR–filter coefficients $c_{h,i}$ are based on the auto–correlation function in time direction. The $L_{a,h,k}$ denote the horizontal *a priori* L–values.

B. Concatenation of two one–dimensional APP estimators

Separate one–dimensional APP estimation in frequency (i.e. vertical) and time (i.e. horizontal) direction is possible owing to the two–dimensional continuity of the channel transfer function. The channel coefficient $a_{k,n}$ does not change abruptly but continuously (smoothly) in time and frequency direction, similar to the situation of a 2D ISI/AWGN–channel studied in [7].

The inputs to the vertical APP estimator are the noise and fading affected channel observations $z_{k,n}$ (i.e. unprocessed discrete–time signal from channel), and *a priori* L–values $L_{a,v}$ (time/frequency indices k, n omitted for L–values) as fed back from the channel decoder. The pilot symbols are included into the APP estimation as "perfect *a priori* knowledge" (i.e. big positive or negative L–value) at the respective positions. For the remaining positions, the vertical *a priori* L–values $L_{a,v}$ are set to zero for the very first pass through the estimator and decoder. The vertical APP estimator outputs the estimated channel L–values $L_{ch,v}$ which are forwarded as *a priori* input $L_{a,h} = L_{ch,v}$ to the horizontal APP estimator. The horizontal APP estimator uses the *a priori* input $L_{a,h}$ and channel observations $z_{k,n}$ to calculate improved horizontal channel L–values $L_{ch,h}$. After subtracting vertical *a priori* knowledge $L_{a,v}$ the signal is passed on to the deinterleaver for further processing in the channel decoder.

Conceptually, $L_{ch,v}$ is *not* statistically independent of the channel observations $z_{k,n}$ (i. e. corrupted by same noise on channel) and thus it does not appear to be suited as *a priori* knowledge $L_{a,h}$ (which is additive, compare to (5)) for the horizontal estimation. However, the resulting noise terms on the vertical and horizontal channel estimates $\hat{a}_{v,n}$, $\hat{a}_{h,k}$ of (4), (6) are independent. It is important to notice that the uncertainty in the channel estimation dominates at the beginning of the iteration (or equivalently, for poor *a priori* and/or channel input) which means that $L_{ch,v}$ stays fairly uncorrelated from $z_{k,n}$ and thus contributes to significantly improve the horizontal estimation if used as *a priori* input. This effect has been verified by the simulations of Section V.

C. Pilot-symbol arrangements

For the APP channel estimation algorithm, the sampling theorem is no longer the crucial criterion to dominate the pilot symbol insertion period, as opposed to e.g. [1]. This is because it can exploit the redundancy of the channel code by iterative estimation and decoding. Hence, the pilot symbol arrangement can be somewhat arbitrary. Preferably the pilot symbols are arranged in a diagonal, interleaved order (rather than aligned to a grid) such that each pilot contributes to improved estimation in both vertical and horizontal direction.

IV. Inserting an inner convolutional code

We can further improve the performance of the iterative decoding loop by inserting an inner rate 1 recursive encoder at the transmitter. Fig. 2 shows the necessary changes at the receiver. Note that the extrinsic information as fed back from the outer decoder first needs to be "transformed" into the inner coded bits domain, such that the estimation stage can also benefit from the new *a priori* knowledge. This transformation is performed by the rate 1 inner decoder, using the *a posteriori* output on the inner coded bits.

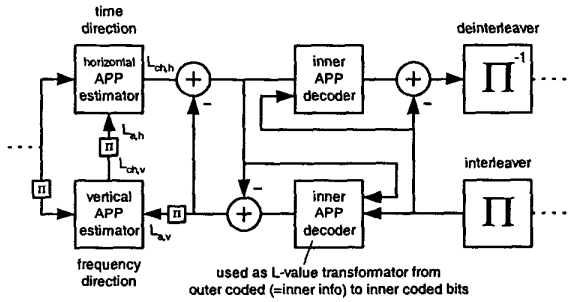

Fig. 2. Modified receiver section with inner APP decoder.

V. Simulation Results

We use the following channel and multicarrier system parameters: duration of one OFDM-symbol $T_s = 300\mu s$, sub-carrier spacing $\Delta f = 4$kHz, channel delay spread $\tau_{max} = 20\mu s$. The maximal Doppler shift is set to $f_D = f_{D,max} = 100$Hz, but varies for different curves in the diagrams to show the influence of the fading rate. With $N = 1000$ adjacent sub-carriers and $K = 100$ consecutive OFDM symbols in time, the interleaving depth is $N \cdot K = 10^5$ outer coded bits.

We noticed that the predictor coefficients $c_{h,i}, c_{v,i}$ of (3), (5) can be chosen in a rather relaxed way, just ensuring to have a low-pass behavior; in our simulations we applied the *pragmatic choice* of $c_{h,i} = 1/m_h, c_{v,i} = 1/m_v$, $\sigma^2_{pred} = \sigma^2_n$.

BER charts are used for performance analysis of different system configurations. In addition to that, we apply the Extrinsic Information Transfer Chart (EXIT chart) [8] to better compare the different estimation algorithms and to gain more insight into the convergence behavior of iterative estimation and decoding.

The outer convolutional code is recursive systematic with feedback polynomial $G_r = 023$, feedforward polynomial $G = 037$ and code rate $R_c = 0.5$. The pilot symbol rate is $R_p = 0.99$, that is, only 1% of the transmitted bits are used as pilot symbols. For APP estimation we chose a diagonal, interleaved pilot symbol arrangement: The discrete time index k of the pilot symbol on sub-carrier n, $0 \le n < N$ is given by $k = (29 \cdot n)\,\mathrm{MOD}\,K$. The conventional Wiener estimator uses a rectangular grid arrangement.

Note that in the following all E_b/N_0-values are given with respect to the overall information rate $R = R_c \cdot R_p = 0.495$.

A. Without inner code

Fig. 3 shows mutual information transfer characteristics of the APP estimation stage. The *a priori* input to the APP estimator is on the abscissa (mutual information $0 \le I_{A_1} \le 1$ in bit per binary symbol). The *a posteriori* (i. e. channel) output is on the ordinate (mutual information $0 \le I_{E_1} \le 1$). Mutual information transfer characteristics describe the input/output relations of the APP estimator and are calculated by applying a Gaussian distributed random variable as *a priori* input and quantifying the *a posteriori* output in terms of mutual information [8].

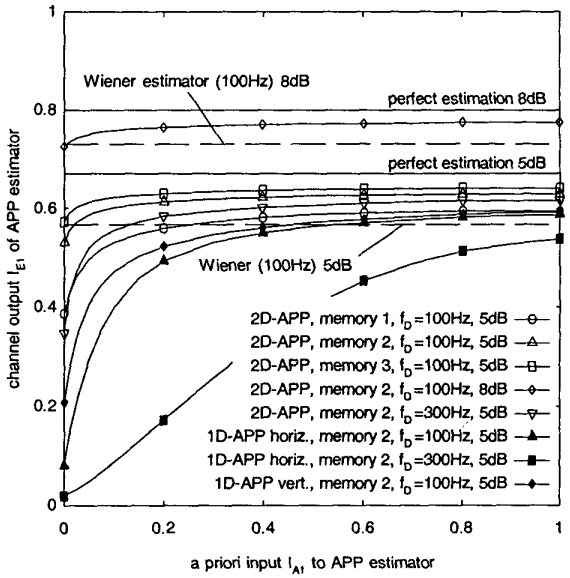

Fig. 3. Mutual information transfer characteristics of APP estimator (one-dimensional, two-dimensional) for different estimator memory and Doppler frequency.

The advantage of using two concatenated one-dimensional APP estimators (2D) in comparison to using a single one-dimensional APP estimator (1D) can clearly be seen: The 2D-curves considerably outperform the 1D-approach for no *a priori* knowledge (very left side of chart) and saturate at higher *a posteriori* output. With increas-

ing *a priori* knowledge I_{A_1}, they almost reach the mutual information of the coherently detected fully interleaved, binary input/continuous output Rayleigh channel with perfect channel knowledge, shown as solid horizontal lines for 5dB (0.67bit, "perfect estimation") and 8dB (0.80bit). For a faster fading of $f_{D,max}$ = 300Hz the gap between 2D and 1D becomes even more pronounced. A higher signal to noise ratio of the channel observations (E_b/N_0 = 8dB instead of 5dB) just raises the estimator transfer characteristic. A smaller estimator memory ($m_h = m_v = 1$) results in weaker *a posteriori* output, whereas a bigger memory ($m_h = m_v = 3$) improves the estimator performance at the cost of additional trellis complexity. For memories greater than 3 (not shown) the performance starts to degrade, as the predictor coefficients are just pragmatically chosen to implement a moving average filter. The estimator performance could be further optimized by taking the time and frequency auto–correlation functions into consideration. However, an estimator memory of 2 already provides good results, and no knowledge of the channel statistics is required.

The dashed horizontal lines depict the reference system applying the conventional FIR–filter interpolation approach ("Wiener estimator") according to [1], using the 11 nearest pilot symbols. It is based on a rectangular pilot symbol grid arrangement with a block size of N = 1001 sub-carriers and K = 101 OFDM–symbols. Hence, every 10th symbol in time and frequency direction is a pilot symbol (1.1% pilot symbols, rather than 1% for the APP estimator case). The filter coefficients are optimized to the channel auto–correlation functions of Section II-B, which are assumed to be perfectly known. Therefore, it is not surprising that the Wiener estimators tend to have a better *a posteriori* output I_{E_1} for no *a priori* knowledge $I_{A_1} = 0$, in comparison to the APP estimators which do not assume any knowledge of the channel statistics.

The APP estimators can overcome the weak beginning of their transfer characteristics by performing iterative estimation and decoding, as illustrated in Fig. 4. The trajectory of iterative decoding shows the exchange of channel and extrinsic information between estimator and decoder in the Extrinsic Information Transfer Chart. The trajectory is a simulation result of the iterative decoding scheme, whereas the transfer characteristics are computed individually for the inner APP estimator and the outer decoder, applying independent Gaussian distributed random variables as *a priori* inputs. Using a big interleaver of 10^5 outer coded bits keeps the correlations of extrinsic information small over several iterations; the trajectory matches with the characteristics fairly well. After about 3 iterations the trajectory gets stuck, owing to the intersection of both characteristics. Note that the estimator transfer characteristics of Fig. 3 are averaged over many multicarrier blocks of $N \cdot K = 10^5$ bits, to level out differences in both the estimation scenarios and the average power of the respective multicarrier blocks. The estimator transfer characteristic of Fig. 4 is computed based on a single block of 10^5 bits, which, obviously, has a weaker start at $I_{A_1} = 0$ than the corresponding averaged characteristic of Fig. 3.

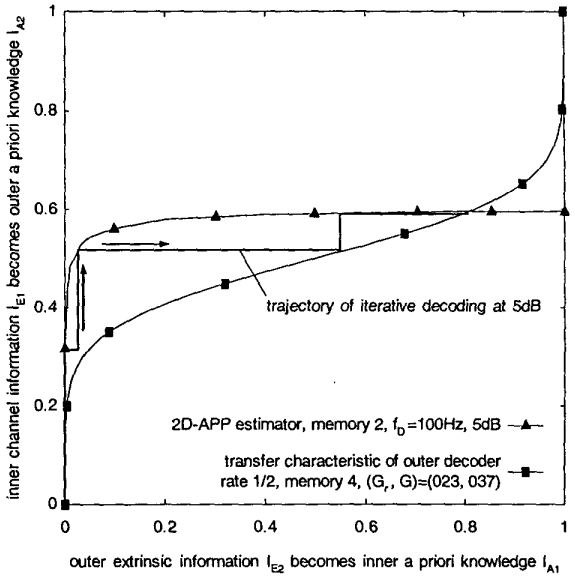

Fig. 4. EXIT chart, two concatenated one–dimensional APP estimators and outer memory 4 decoder with simulated trajectory of iterative decoding at E_b/N_0 = 5dB.

The BER chart of Fig. 5 shows the performance improvement by using APP estimation in comparison to the FIR–interpolation method of the reference system. At f_D = 100Hz the advantage is about 1dB (BER 10^{-4}). At f_D = 200Hz > 167Hz the Wiener estimator fails, as the pilot symbol spacing does no longer fulfill the the sampling theorem. The APP estimator, however, can tolerate even higher fading rates, or equivalently, requires less pilot symbols. For f_D = 300Hz, the cliff of the iterative BER reduction moves slightly towards higher E_b/N_0. The robustness of the APP estimation algorithm is remarkable if we keep in mind that the Wiener filter was designed assuming perfect knowledge of the channel auto–correlation functions, whereas the filter coefficients of the APP estimator are just pragmatically chosen (see beginning of this Section), not relying on the knowledge of the channel statistics.

B. With inner code

The iterative estimation and decoding loop of the system with inner decoder can be studied in the EXIT charts of Fig. 6. We chose a rate 1 memory 1 inner recursive convolutional encoder at the transmitter, with polynomials $G_r = 03, G = 02$ (i. e. a differential encoder). The inner transfer characteristics almost reach the point $(I_{A_1}, I_{E_1}) \approx (1, 1)$, indicating that a low BER can be achieved by means of iterative decoding.

The BER curves of Fig. 7 show a steep "turbo cliff" with a low BER floor on the right side of the BER chart. After simulating 10^7 information bits we did not measure any errors in the BER floor region. At a BER of 10^{-4} and f_D = 100Hz the advantage to the reference system is

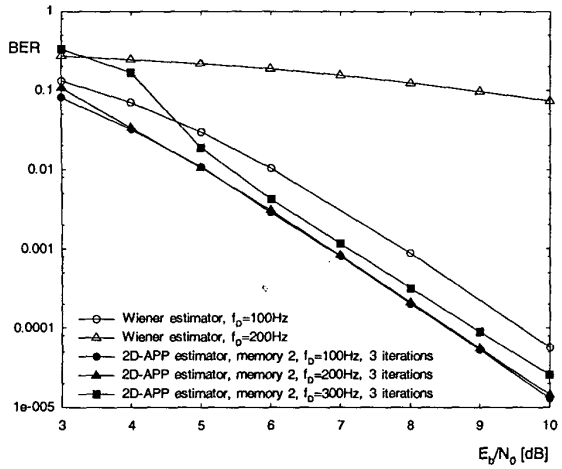

Fig. 5. BER curves of APP estimation in comparison with reference curves of conventional FIR–interpolation method.

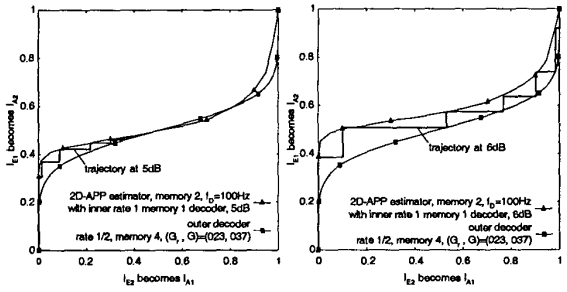

Fig. 6. EXIT charts of APP estimator and inner rate one convolutional decoder in combination with outer memory 4 decoder; decoding trajectories at $E_b/N_0 = 5$dB (left) and 6dB (right).

about 4dB. Note that the EXIT chart on the left hand side of Fig. 6 depicts the convergence situation just before the turbo cliff (5dB); the EXIT chart on the right hand side is taken at an E_b/N_0–value right after the cliff (6dB), with the iterative decoding trajectory climbing up to $(I_{A_1}, I_{E_1}) \approx (1, 1)$. The EXIT chart predictions on iterative decoding convergence have shown to yield very accurate results for the case of code design on AWGN channels, e. g. [8], [9]. However, for iterative estimation and decoding on Rayleigh fading channels the trajectories slightly miss the transfer characteristics (Fig. 6); a more careful modelling of *a priori* knowledge (rather than Gaussian) could help to improve the prediction accuracy.

VI. Conclusions

We have shown that two–dimensional channel estimation for coherent detection of OFDM signals can be performed by a concatenation of two one–dimensional APP estimators. The new channel estimation algorithm turns out to be more robust against changes in the channel statistics than the conventional FIR–interpolation approach, in particular

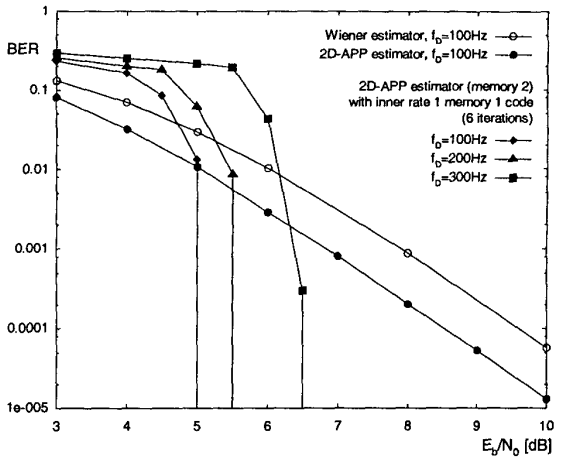

Fig. 7. BER chart of the system with inner decoder; for better comparison, two reference curves are copied from Fig. 5.

by benefiting from the opportunity of performing iterative estimation and decoding. A combination with an inner rate one recursive convolutional code further improves the performance of the iterative estimation and decoding loop.

References

[1] P. Hoeher, S. Kaiser, P. Robertson, "Two–dimensional pilot–symbol–aided channel estimation by Wiener filtering", *Proc. ICASSP*, pp. 1845–1848, April 1997

[2] P. Hoeher, J. Lodge, "Iterative Differential PSK Demodulation and Channel Decoding", *IEEE Trans. Comm.*, vol. 47, pp. 837-843, June 1999

[3] L. Bahl, J. Cocke, F. Jelinek, J. Raviv, "Optimal decoding of linear codes for minimizing symbol error rate", *IEEE Trans. Inform. Theory*, vol. 20, pp. 284–287, Mar. 1974

[4] P. Hoeher, "A Statistical Discrete-time model for the WSSUS multipath channel", *IEEE Trans. Comm.*, vol 41, pp. 461-468, Nov. 1992

[5] J. Hagenauer, E. Offer, L. Papke, "Iterative Decoding of Binary Block and Convolutional Codes", *IEEE Trans. Inform. Theory*, vol. 42, no. 2, pp. 429–445, Mar. 1996

[6] J. H. Lodge, M. L. Moher, "Maximum likelihood sequence estimation of CPM signals transmitted over Rayleigh flat–fading channels", *IEEE Trans. Comm.*, vol 38, no. 6, pp. 787–794, June 1990

[7] X. Chen, K. M. Chugg, "Near-optimal data detection for two–dimensional ISI/AWGN channels using concatenated modeling and iterative algorithms", *Proc. ICC*, pp. 952–956, 1998

[8] S. ten Brink, "Iterative Decoding Trajectories of Parallel Concatenated Codes", *Proc. 3rd IEEE/ITG Conference on Source and Channel Coding*, pp. 75–80, Munich, Jan. 2000

[9] S. ten Brink, "A rate one–half code for approaching the Shannon limit by 0.1dB", *Electron. Lett.*, vol. 36, no. 15, pp. 1293–1294, July 2000